Electrochimica Acta 173 (2015) 607–612

Contents lists available at ScienceDirect

Electrochimica Acta

journal homepage: www.elsevier.com/locate/electacta

Co-sensitization of TiO_2-MWCNTs hybrid anode for efficient dye-sensitized solar cells

Umer Mehmood [a], Shakeel Ahmed [b], Ibnelwaleed A. Hussein [a,*], Khalil Harrabi [c]

[a] Department of Chemical Engineering, King Fahd University of Petroleum & Minerals, P. O. Box 5050, Dhahran, 31261, Kingdom of Saudi Arabia
[b] Center for Refining & Petrochemicals, King Fahd University of Petroleum & Minerals, Dhahran, 3161, Kingdom of Saudi Arabia
[c] Department of physics, KFUPM, P. O. Box 5050, Dhahran, 31261, Kingdom of Saudi Arabia

ARTICLE INFO

Article history:
Received 13 April 2015
Received in revised form 20 May 2015
Accepted 22 May 2015
Available online 28 May 2015

Keywords:
Hybrid
multi-walled carbon nanotubes
co-sensitization
density functional theory

ABSTRACT

Co-sensitization of dyes on hybrid TiO_2- MWCNTs photoanode is an effective approach to enhance the performance of a dye-sensitized solar cell (DSSC). In this work, N719 sensitizer is co-sensitized with N3. The co-sensitized device showed enhanced V_{OC} and J_{SC} in comparison to single-dye sensitized devices. Upon optimization, the device made of the 0.1Mm N_3 + 0.4 mM N719 yielded J_{SC} = 12.5 mA cm^{-2}, V_{oc} = 0.73 V, FF = 0.45 and η = 4.1 %.This performance is superior to that of either of the individual DSSCs sensitized with N3 (3.69%) and N719 (3.51 %) under the same conditions of fabrication. The efficiency of DSSCs was further improved to 4.46% by the incorporation of MWCNTs in TiO_2. The hybrid TiO_2/MWCNTs photoanodes with different concentrations of CNTs (0.04. 0.08, 0.12, 0.16 wt. %) were prepared using mixing technique. The optimized molar ratio of N3/N719 was used for the sensitization of hybrid photonodes. Density functional theory (DFT) was used to compute the band gaps of TiO_2 and CNT-TiO_2 clusters.

1. Introduction

Energy is the driving force for development, economic growth, automation, and modernization. Energy usage and demand are increasing globally and researchers have taken this seriously to fulfill future energy demands [1,2]. At present global energy sources are mainly dependent on fossil fuels and the use of fossil fuel is the main reason for global increases of CO_2 amount [3]. According to global carbon emissions sources [4], carbon dioxide emissions from coal, oil, natural gas, cement, and gas flaring were 43%, 33%, 18%, 5.3%, and 0.6%, respectively in 2012. Emissions of greenhouse gases grew 2.2% per year between 2000 and 2010, compared with 1.3% per year from 1970 to 2000 [5]. The world is not capable of absorbing large amounts of CO_2 at the rate it is produced by fossil fuels. As a result, increasing the volume of CO_2 in the environment has increased global warming and further climate change. Global warming and climate changes are challenging all over the world. The use of renewable energy provides benefits that reduce emissions of air pollutants as well as greenhouse gases . Therefore, alternative sources of energy are needed so that mankind can survive on the earth without depending on fossil fuels. Solar energy is one of the renewable energy sources that will contribute to the security of future energy supplies [6,7]. Solar radiation from the sun is approximately 3×10^{24} J per year, which is ten times the current energy demands [8]. Light from the sun can be harvested by dye-sensitized solar cells (DSSCs). DSSCs have attracted considerable attention due to an ideal compromise between efficiency and cost-performance [9–11].The major component of the DSSCs is a dye. Its function is to absorb incoming sunlight and produce excitons. It is chemically bonded to the porous surface of the semiconductor.

However, the traditional dyes generally used in DSSCs suff ; ;er from narrow absorption spectra and/or low absorption intensity and therefore low efficiency of DSSCs [10]. To achieve higher cell efficiency, a certain sensitizer is needed so as to absorb incident light as much as possible., Currently, there is no single organic sensitizer which provides strong absorption in a wide range of wavelengths (400-900 nm) [12]. Therefore, the co - sensitization strategy is applied to the organic dyes with complementary absorption spectra to obtain a broader and a more intense absorption band, thus increasing the performance of the DSSC [13–15]. Many co-sensitization systems have been proposed and demonstrated improved photovoltaic performance, such as ruthenium complex co-sensitized with an organic dye [16–18], porphyrin [19–21] or phtalocyanine [22–24] co-sensitized with an organic dye, and organic dye co-sensitized with another organic

* Corresponding author.
E-mail address: ihussein@kfupm.edu.sa (I.A. Hussein).

http://dx.doi.org/10.1016/j.electacta.2015.05.132
0013-4686/

dye [25,26]. Another major cause of low efficiency of DSSCs is the recombination of injected electrons with the electrolyte (dark current) [27]. The incorporation of CNTs in TiO_2 films may improve the electron transport in DSSCs [28–30], owing to the creation of complex interpenetrating networks and favorable electrical conductivity [31,32]. It is supposed that one-dimensional carbon nanostructures allow the photocurrent to flow more efficiently in DSSCs by increasing orientation orders.

In this work both approaches (co-sensitization and hybrid anode) were used simultaneously to improve the efficiency of DSSCs. Here, we also employed DFT to find the band gaps. It is an effective tool as compared to other high level quantum approaches because the computed orbitals are suitable for the typical MO-theoretical analyses and interpretations [33].

2. Computer simulation

All the DFT calculations were executed using Amsterdam Density Functional (ADF) program (2013.01). BAND mode was used to simulate the anatase TiO_2 clusters. The tetragonal anatase crystal structure was selected with single layer (001) surface slab [34]. Then, we created 4×1 super cell from this slab. All atoms were mapped within the unit cell.TiO_2 and CNTdoped TiO_2 models were simulated by considering hybrid at Becke parameter, Lee-Yang-Parr (BYLP) level and triple-ζ polarization basis function. In all the calculations, the relativistic effects were taken into account by the zero order regular approximation (ZORA) Hamiltonian in its scalar approximation [35].

3. Experimentation

Seven different samples of N3,N719 and N3 + N719 i.e. 0.5 mM N3, 0.4 mM N3 + 0.1 mM N719, 0.3 mM N3 + 0.2 mM N719, 0.25 mM N3 + 0.25 mM N719, 0.2 mM N3 + 0.3 mM N719, 0.1 mM N3 + 0.4 mM N719 and 0.5 mM N719 were prepared in methanol. DSSCs (TiO_2 based) were first fabricated (in open atmosphere) using these co-sensitization systems and then characterized to find the best system. The best co-sensitization system was then employed in hybrid TiO_2-MWCNTs based DSSCs to further improve the efficiency/performance.

3.1. Preparation of composite anodes

A suspension of ethanol and MWCNTs was prepared by dissolving 30 mg of MWCNTs (OD 10-20 μm, purity > 95%, Ash <1.5%) in 25 ml ethanol. It was then sonicated for 4hr to attain a good dispersion of MWNTs in ethanol. An exact quantity of dispersed MWCNTs was mixed with known amount of anatase TiO_2 paste (T/SP **14451**, Solaronix) to obtain a composite paste. Five different samples of TiO_2-MWCNTs were prepared by varying the composition of MWCNTs i.e. 0, 0.04. 0.08, 0.12, 0.16 wt. %. The TiO_2-MWCNTs paste was then tape casted on FTO glass substrate (2 mm, 7 Ω/seq, Solaronix). The coated glass substrate was annealed at 450 °C for 30 min. Other photoanodes were prepared following the same procedure. The thickness of each photoanode was found by using cross sectional images obtained from SEM (JEOL, 6610LV). The average thickness of each film was 22 μm.

3.2. Fabrication of DSSCs

TiO_2 and TiO_2-MWCNTs electrodes were soaked in the dye solutions for 24 h. After sensitization, the samples were washed with ethanol to eliminate unanchored dye. Then, DSSCs were fabricated employing the sensitized anode (TiO_2, MWCNTs-TiO_2), platinum deposited counter electrode (Plasticol T, Solaronix), 60 μm sealing spacer (Meltonix 1170, Solaronix) and I^-/I_3^- redox couple electrolyte prepared in methoxypropionitrile with a 50 mM redox concentration (Iodolyte Z-50, Solaronix). The active surface area of the solar cell was 0.35 cm^2.

3.3. Characterization of DSSCs

The UV-vis spectra of dye solutions in methanol and adsorbed on TiO_2 and MWCNTs-TiO_2 films at glass substrates were recorded with JASCO-670 UV/VIS spectrophotometer. Keithley 2400 Source Meter was used to measure the $I–V$ characteristics of the DSSCs using IV-5 solar simulator (Sr #83, PV Measurement, Inc) at AM1.5G (100 mWcm^{-2}). The silicon solar cell was used as a reference for calibration. The impedance spectroscopy (EIS) was measured in dark conditions of illumination via Bio-Logic SAS (VMP3, s/n:0373), with an AC signal of 10 mV in amplitude, in the frequency range between 10 Hz and 1 MHz.

4. Results and Discussion

4.1. Morphological properties of composite anode

The dispersion of MWCNTs in TiO_2 was observed by TEM (JEOL, JEM-2100F) analysis. TiO_2-MWCNT sample having 0.16% CNT was

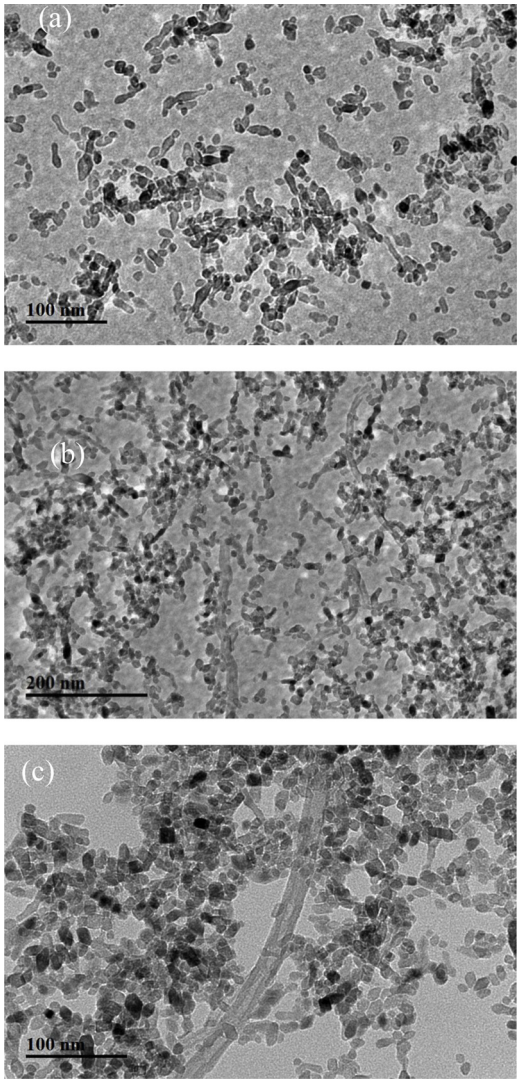

Fig. 1. *TEM* images of a 0.16 % sample (a) Pure TiO_2 b) Dispersion of MWCNTs in TiO_2 and c) Dispersion of single MWCNT in TiO_2.

selected for TEM analysis, because it was difficult to obtain TEM images of dispersed MWCNTs in TiO_2 from low concentration samples. Fig. 1(b) shows that the CNTs are well dispersed in TiO_2, although a few tangles can be observed due to the length of the MWCNTs. The interface connection between MWCNTs and TiO_2 can clearly be observed, indicating that TiO_2 possesses good affinity with MWCNTs. The inner core is hardly visible, because the surface of MWCNT is well decorated with TiO_2 nanoparticles as shown in Fig. 1(c).

Table 1
Simulated electronic structure properties of TiO_2 and CNT doped TiO_2.

System	E_{CB} (eV)	V_B (eV)	Band gap (eV)
TiO_2	−4.10	−7.20	3.10
CNT-TiO_2	−4.40	−6.45	2.01

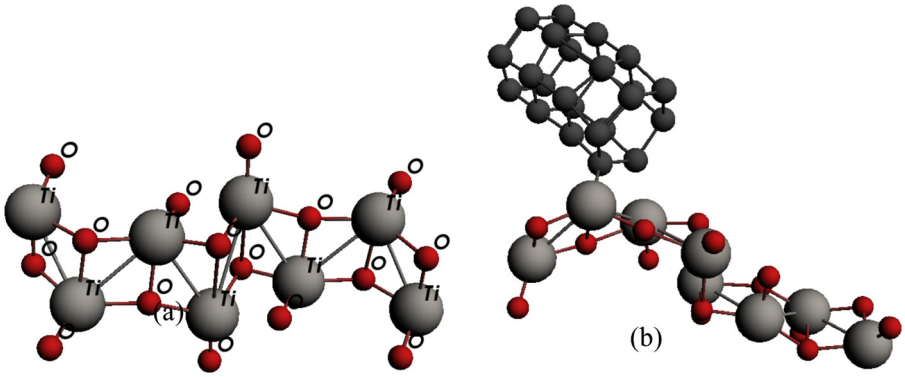

Fig. 2. Simulated structures of TiO_2 (a) and carbon doped TiO_2.

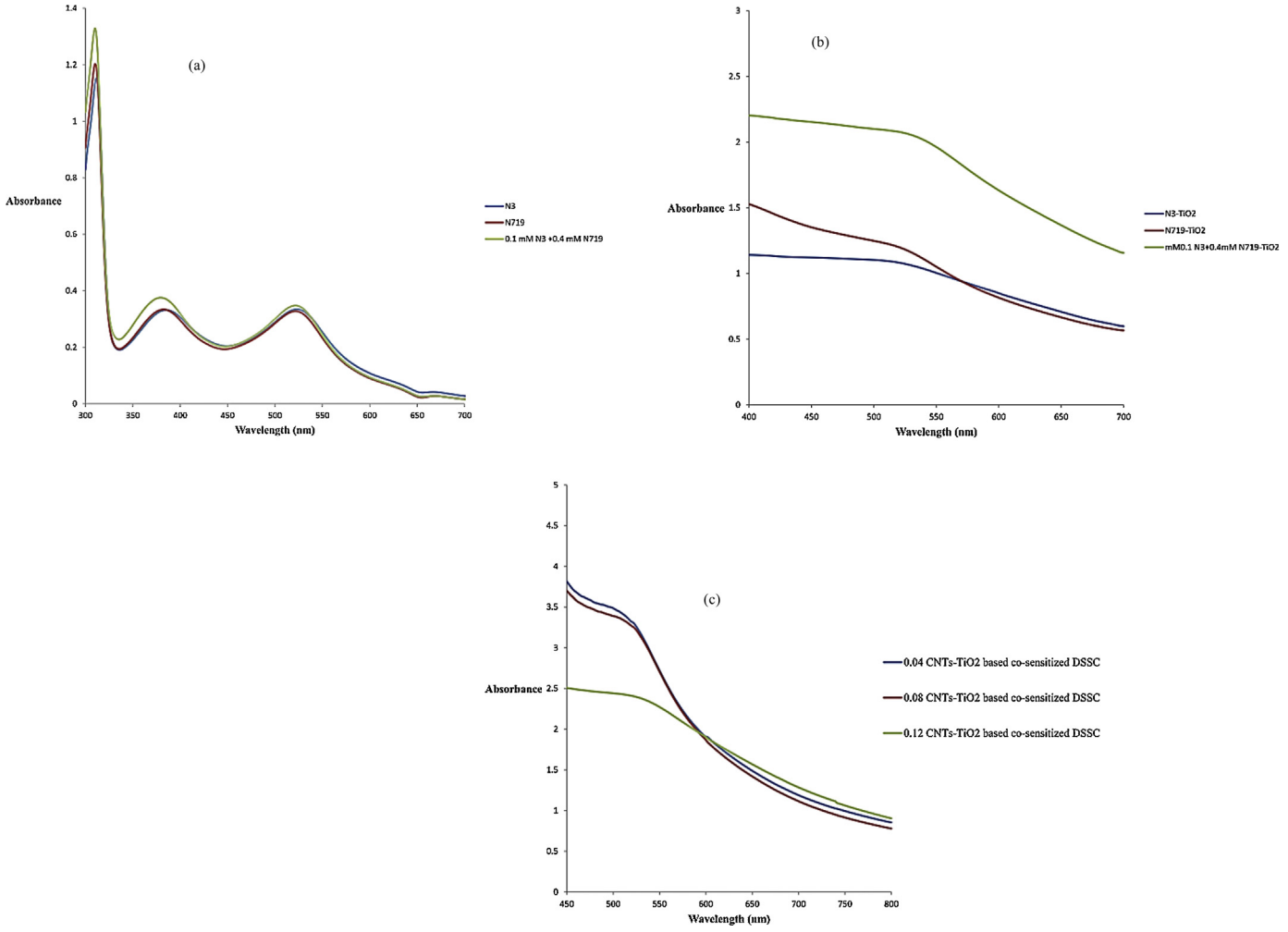

Fig. 3. (a). UV-vis spectra of a) pure dyes in solvent b) Dyes anchored to TiO_2 film and c) dye anchored to MWCNTs-TiO2 hybrid composite film.

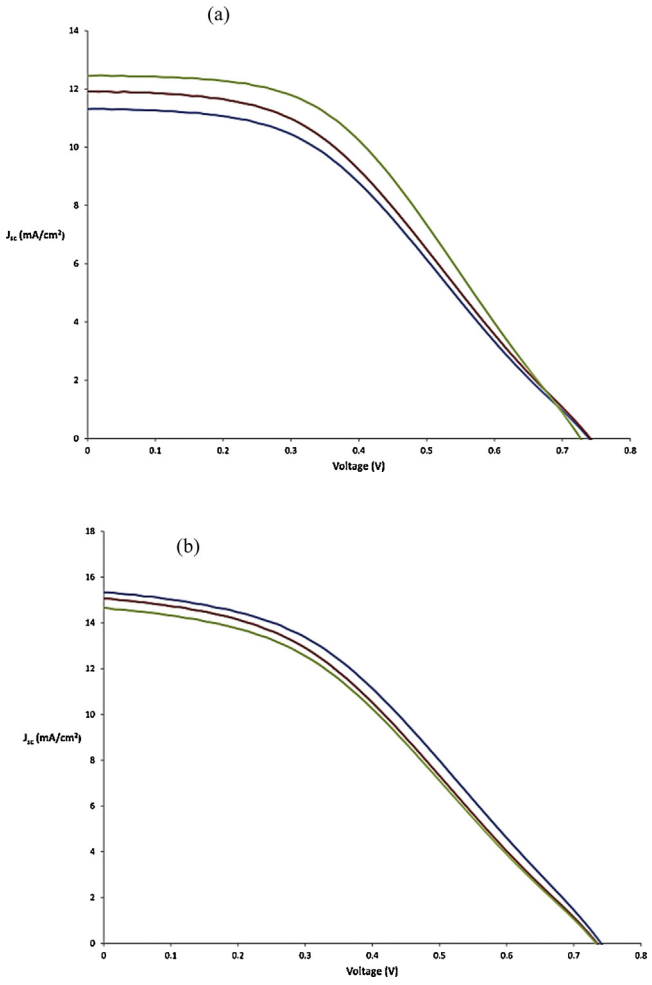

Fig. 4. Current – voltage characteristics of DSSCs fabricated using a) TiO_2 and b) MWCNTs-TiO_2.

4.2. Electrochemical properties

The HOMOs, LUMOs and band gap energies of photosensitizers play an important role in providing the thermodynamic driving force for the electron injection to the conduction band of TiO_2. For efficient charge transfer, the LUMOs of dyes must be more negative than the conduction band of the semiconductor while HOMO levels must be more positive than the redox potential of electrolyte. The simulated structures of TiO_2 and CNT-TiO_2 are shown in Fig. 2. The simulated conduction band, valence band and band gap of TiO_2 and CNT-TiO_2 are shown in Table 1. These tabulated values are in good agreement with the experimental values [36]. The computed results show that doping of MWCNTs on TiO_2 significantly reduces the band gap of TiO_2 cluster. This is because the CNTs possess the lower value of the ECB (~0 EV vs. NHE) than that of TiO_2 (−0.5 eV vs. NHE) [29]. The charge equilibrium between CNTs and TiO_2 would cause a shift of apparent Fermi level to more positive potential i.e.downward potential. The downward positive shift due to MWCNTs can cause a significant driving force to expedite the charge transport from the dye to the photoanode.

4.3. Optical properties

UV-Vis spectra of N719, N3 and N719 + N3 are shown in Fig. 3(a). N3 and N719 share similar absorption spectra as well as molecular structures. The broad visible peaks at 528, 526 and 382, 384 nm in N719 and N3 respectively, are assigned to metal-to-ligand charge transfer (MLCT) origin. The bands in the UV at 314,312 nm are assigned as intra ligand (π-π^*) charge-transfer transitions. High absorption is observed for overall wavelengths in the absorption spectrum of 0.1 mM N3 + 0.4 mM N719 due to the synergistic effect of the two dyes.But less pronounced enhancement in the absorption peak hight indicates lower probability of hydrogen bond formation between the two dyes. However, the absorption spectrum of 0.1 mM N3 + 0.4 mM N719 shifts to lower energy values when anchored to TiO_2, shown in Fig. 3(b). It is due to the binding of the carboxylate groups (from both dyes) to the TiO_2 surface in which Ti^{4+}acts as proton. The interaction between the carboxylate groups and the surface Ti^{4+}ions may lead to increased delocalization of the π^* orbital. The energy of the π^* level is decreased by this delocalization, which explains the red shift for the absorption spectrum. Moreover, the absorption spectrum of TiO_2/N3 + N719 is more intense and broader as compared to individual dyes anchored to TiO_2. It means that the proposed co-sensitized thin films can absorb more photons than the individual sensitized TiO_2 films. Similarly, the co-sensitized based MWCNTs-TiO_2 thin films show high absorption as compared to TiO_2 co-sensitized film, shown in Fig. 3(c). This is because the CNTs may exhibit photosensitizing properties, thus extending photovoltaic properties into the visible spectrum [37]. However, the further increase in CNTs contents from an optimum level (0.04%) decreases the absorption of co-sensitized films (0.08% and 0.12%) due to diminution in film transparency.

4.4. Photovoltaic performance

Fig. 4(a) shows the current-voltage (*I-V*) characteristics of the TiO2 based DSSCs, sensitized/co-sensitized by N719,N_3 and N_3 + N719. While Fig. 4(b) shows the (*I-V*) characteristics of the hybrid photoanode MWCNTs-TiO_2 based DSSCs, co-sensitized by 0.1 mM N3 + 0.4 mM N719. The photovoltaic parameters of DSSCs, i.e. J_{sc}, V_{oc}, series resistance (R_s), Shunt resistance (R_{sh}) and FF are shown in Table 2. Under a standard AM 1.5G simulated sunlight irradiation, the N719 sensitized DSSC gave a J_{sc} of 11.31 mA·cm^{-2}, a

Table 2
Photovolatic properties of DSSCs.

DSSCs	j_{sc} (mA/cm^2)	V_{oc} (mV)	FF(%)	η (%)	R_s(Ω)	R_{sh}(Ω)
TiO_2/0.5 mM N719	11.312	739	42.00	3.51	217	549
TiO_2/0.5 mM N3	11.970	741	41.77	3.69	208	889
TiO_2/0.4 mM N719 + 0.1 mM N3	12.500	727	45.30	4.10	204	453
TiO_2/0.3mM N719 + 0.2 mM N3	13.700	742	39.70	4.00	178	817
TiO_2/0.25mM N719 + 0.25mM N3	12.219	750	41.65	3.81	208	1203
TiO_2/0.20 mM N719 + 0.30 mM N3	12.731	760	40.50	3.90	196	1330
TiO_2/0.1 mM N719 + 0.4 mM N3	12.801	744	38.30	3.65	192	595
0.04%CNTS-TiO_2/0.4 mM N719 + 0.1 mM N3	15.331	741	39.25	4.46	158	1260
0.08%CNTS-TiO_2/0.4 mM N719 + 0.1 mM N3	15.059	734	38.10	4.21	158	1080
0.12%CNTS-TiO_2/0.4 mM N719 + 0.1 mM N3	14.700	731	38.25	4.12	161	1040

V_{oc} of 739 mV, and a FF of 41.98%, resulted in an efficiency of 3.51%. Moreover, the N3 sensitized DSSC yielded a J_{sc} of 12 mA·cm^{-2}, a V_{oc} of 741 mV, a FF of 42%, and a efficiency of 3.7%. Encouragingly, compared with the devices sensitized by N3 or N719 alone, the co-sensitized (N3 + N719) DSSC exhibited a significantly improved efficiency of 4.10%. The improvement in the efficiency is mainly due to the enhancement of the J_{SC} values (14.2 mA·cm^{-2}), which are highly related to the range and the intensity of the absorption spectrum. The overall efficiency of DSSCs was further improved to 4.46% by the incorporation of MWCNTs in TiO_2. Insertion of MWCNTs in TiO_2 network significantly enhances the efficiency of DSSC. This is because the incorporation of MWCNTs: a) increases the surface area of hybrid anode and thus more dye loading, b) enhances light harvesting efficiency and thus more photo current and henec more efficiency and c) improve the electron injection efficiency of the electrons due to increase positive potential (as described above in sec-4.2). The little decline in V_{oc} at increasing CNTs contents could be attributed to the downshift of the potential band edge of the TiO_2. As FF depends on both Rs (should be low) and R_{sh} (should be high), the FF values are low for these DSSCs (Table 2) which is supported by the measured high Rs and low Rsh values (Table 2). The low shunt resistance causes power losses in solar cells by providing an alternate pathway for the light-generated current, which lowers FF. R_{sh} should be of the order of $10^3\ \Omega$ for a highly efficient solar cell [37]. The high series resistance (Rs) is mainly due to large thickness of platinum counter electrode or electrolyte layer [38,39]. While low shunt resistance (R_{sh}) can be attributed to an inefficient fabrication process of DSSCs [40].

However an increase in MWCNTs concentration from an optimum level (0.04%) negatively affects the performance of DSSCs owing to decrease in film transparency. Another possibility of low efficiency at a high MWCNTs concentration could be attributed to the formation of CNT agglomerates inside the TiO_2 matrix acting as trapping sites that obstruct the fast charge collection at the electrodes. Therefore, the poor charge collection at the photoanode and light losses due to CNT direct absorption, diminish the efficiency of DSSCs at high CNTs contents.

4.5. Electrochemical impedance spectroscopy (EIS) analysis

EIS analysis is performed to further elucidate the photovoltaic properties. Fig. 5 shows the Nyquist plot of DSSCs which were assembled with N719,N3, 0.1 mM N3 + 0.4 mM N719 and hybrid CNTs-TiO_2 co-sensitized. Generally, a normal impedance spectra of DSSCs is represented by three arcs (semicircles). The first semicircle represents the inter face resistance of electrons at counter electrode/electrolyte (R_1), second signifies the interface resistance at the photoanode / electrolyte (R_2), and the third indicates the diffusion process of I^-/I_3^- redox couple in electrolyte (*Zw*) [41,42]. Only second arc comes out in the Nyquist plot in the Fig 5. It is probable that the other two arcs corresponding to R_1 and *Zw* are overshadowed by large semicircle reprenting R_2 [43,44]. The R_2 is related to the charge recombination rate, e.g., a smaller R_2 indicates a faster charge recombination. It can be clearly seen in Fig. 5 that the radius of the semicircle for 0.1 mM N3+0.4 mM N719 based DSSC is greater than the based on the single dye and therefore possess high electron life time. The longer electron lifetime for DSSC based on cosensitization may be either due to a higher surface coverage of dye on the TiO_2 surface after cosensitization that block the approach of I_3^- to the free TiO_2 surface and decrease the recombination of injected electron with I_3^- ions, or due to the less aggregation of individual dyes in cosensitized conditions that improves the electron injections. Reduction in charge recombination and electron life time were further improved by the incorporation of MWCNTs in TiO_2. The R_2 value for TiO_2/0.1Mm N_3 + 0.4 mM N719 is smaller than that of 0.04% MWCNTs-TiO_2/0.1Mm N_3 + 0.4 mM N719 DSSC, proposing charge recombination is greatly reduced owing by incorporation of CNTs. However, the CNTs concentration greater than 0.04 wt.% will lead to the smaller values of R_3 due to a shorter electron lifetime of electrons [30].

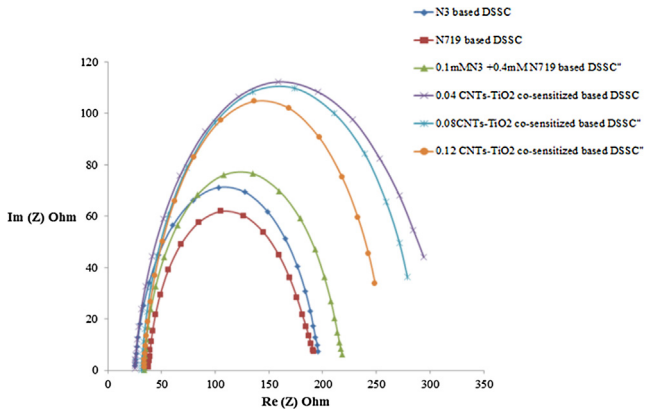

Fig. 5. EIS investigation of TiO_2 and TiO_2-MWCNTs based DSSCs.

5. Conclusion

The mixed solution of N719 and N3 in methanol was used for the co-sensitization of the photoanodes of DSSCs. The absorption spectrum of the co-sensitized TiO_2 films becomes more intense and broader than the absorption spectra of the individual N719 and N_3 dyes. The results indicate that the power conversion efficiency of DSSC based on 0.4N719 + 0.1N_3 is 17% and 11% higher than based on the individual dyes N719 and N3 respectively. Moreover, the cell efficiency of the DSSC with a molar ratio of N3/N719 = 0.1/0.4 was further improved to 4.46% by the incorporation of MWCNTs in TiO_2. Optimum concentration (0.04%) of CNTs in photoanode does not aff ; ;ect the transparency of TiO_2 layer, while significantly increases the PCE of DSSC. Thus, we established a fast and highly eff ; ;ective technique to enhance the light conversion efficiency of DSSCs.

Acknowledgement

The authors would like to acknowledge the support provided by King Abdulaziz City for Science and Technology (KACST) through the Science & Technology Unit at King Fahd University of Petroleum & Minerals (KFUPM) for funding this work through project # 11-ENE1635-04 as part of the National Science, Technology and Innovation Plan. KFUPM is also acknowledged for supporting this research. The authors would like to acknowledge the Center of Research Excellence for Renewable Energy at KFUPM.

References

[1] M. Hasanuzzaman, N.A. Rahim, R. Saidur, S.N. Kazi, Energy savings and emissions reductions for rewinding and replacement of industrial motor, Energy 36 (2011) 233–240, doi:http://dx.doi.org/10.1016/j.energy.2010.10.046.
[2] M. Hasanuzzaman, N.A. Rahim, M. Hosenuzzaman, R. Saidur, I.M. Mahbubul, M.M. Rashid, Energy savings in the combustion based process heating in industrial sector, Renew. Sustain. Energy Rev. 16 (2012) 4527–4536, doi:http://dx.doi.org/10.1016/j.rser.2012.05.027.
[3] G.R. Timilsina, S. Csordás, S. Mevel, When does a carbon tax on fossil fuels stimulate biofuels? Ecol. Econ. 70 (2011) 2400–2415, doi:http://dx.doi.org/10.1016/j.ecolecon.2011.07.022.
[4] J.G. Canadell, C. Le Quéré, M.R. Raupach, C.B. Field, E.T. Buitenhuis, P. Ciais, et al., Contributions to accelerating atmospheric CO2 growth from economic activity, carbon intensity, and efficiency of natural sinks., Proc, Natl. Acad. Sci. U. S. A. 104 (2007) 18866–18870, doi:http://dx.doi.org/10.1073/pnas.0702737104.

[5] M. Hosenuzzaman, N.A. Rahim, J. Selvaraj, M. Hasanuzzaman, A.B.M.A. Malek, A. Nahar, Global prospects, progress, policies, and environmental impact of solar photovoltaic power generation, Renew, Sustain. Energy Rev. 41 (2015) 284–297, doi:http://dx.doi.org/10.1016/j.rser.2014.08.046.

[6] K.W.J. Barnham, M. Mazzer, B. Clive, Resolving the energy crisis: nuclear or photovoltaics? Nat. Mater. 5 (2006) 161–164, doi:http://dx.doi.org/10.1038/nmat1604.

[7] J.-L. Bredas, J.R. Durrant, Organic photovoltaics, Acc. Chem. Res. 42 (2009) 1689–1690, doi:http://dx.doi.org/10.1021/ar900238j.

[8] A. Hussein and B.V.S.R. Umer Mehmood, Saleem-ur Rahman, Khalil Harrabi, Ibnelwaleed A. Hussein, Recent Advances in Dye Sensitized Solar Cells, Adv. Mater. Sci. Eng. 2014 (2014) 12. http://dx.doi.org/10.1155/2014/974782

[9] N. Robertson, Optimizing dyes for dye-sensitized solar cells, Angew. Chem. Int. Ed. Engl. 45 (2006) 2338–2345, doi:http://dx.doi.org/10.1002/anie.200503083.

[10] A. Hagfeldt, G. Boschloo, L. Sun, L. Kloo, H. Pettersson, Dye-sensitized solar cells, Chem. Rev. 110 (2010) 6595–6663, doi:http://dx.doi.org/10.1021/cr900356p.

[11] C. Klein, M.K. Nazeeruddin, P. Liska, D. Di Censo, N. Hirata, E. Palomares, et al., Engineering of a novel ruthenium sensitizer and its application in dye-sensitized solar cells for conversion of sunlight into electricity, Inorg. Chem. 44 (2005) 178–180, doi:http://dx.doi.org/10.1021/ic048810p.

[12] J.-H. Yum, S.-R. Jang, P. Walter, T. Geiger, F. Nüesch, S. Kim, et al., Efficient co-sensitization of nanocrystalline TiO (2) films by organic sensitizers, Chem. Commun. (Camb). (2007) 4680–4682, doi:http://dx.doi.org/10.1039/b710759e.

[13] S.-Q. Fan, C. Kim, B. Fang, K.-X. Liao, G.-J. Yang, C.-J. Li, et al., Improved Efficiency of over 10% in Dye-Sensitized Solar Cells with a Ruthenium Complex and an Organic Dye Heterogeneously Positioning on a Single TiO 2 Electrode, J. Phys. Chem. C. 115 (2011) 7747–7754, doi:http://dx.doi.org/10.1021/jp200700e.

[14] L. Wei, Y. Yang, R. Fan, Y. Na, P. Wang, Y. Dong, et al., N,N'-Bis((6-methoxylpyridin-2-yl) methylene)-p-phenylenediimine based d(10) transition metal complexes and their utilization in co-sensitized solar cells, Dalton Trans. 43 (2014) 11361–11370, doi:http://dx.doi.org/10.1039/c4dt00437j.

[15] Y. Ogomi, S.S. Pandey, S. Kimura, S. Hayase, Probing mechanism of dye double layer formation from dye-cocktail solution for dye-sensitized solar cells, Thin Solid Films 519 (2010) 1087–1092, doi:http://dx.doi.org/10.1016/j.tsf.2010.08.049.

[16] H. Ozawa, R. Shimizu, H. Arakawa, Significant improvement in the conversion efficiency of black-dye-based dye-sensitized solar cells by cosensitization with organic dye, RSC Adv. 2 (2012) 3198, doi:http://dx.doi.org/10.1039/c2ra01257j.

[17] L. Wei, Y. Yang, R. Fan, P. Wang, L. Li, J. Yu, et al., Enhance the performance of dye-sensitized solar cells by co-sensitization of 2 6-bis(iminoalkyl) pyridine and N719, RSC Adv. 3 (2013) 25908, doi:http://dx.doi.org/10.1039/c3ra44194f.

[18] S.P. Singh, M. Chandrasekharam, K.S.V. Gupta, A. Islam, L. Han, G.D. Sharma, Co-sensitization of amphiphilic ruthenium (II) sensitizer with a metal free organic dye: Improved photovoltaic performance of dye sensitized solar cells, Org. Electron. 14 (2013) 1237–1241, doi:http://dx.doi.org/10.1016/j.orgel.2012.12.014.

[19] A. Yella, H.-W. Lee, H.N. Tsao, C. Yi, A.K. Chandiran, M.K. Nazeeruddin, et al., Porphyrin-sensitized solar cells with cobalt (II/III)-based redox electrolyte exceed 12 percent efficiency, Science. 334 (2011) 629–634, doi:http://dx.doi.org/10.1126/science.1209688.

[20] C.-M. Lan, H.-P. Wu, T.-Y. Pan, C.-W. Chang, W.-S. Chao, C.-T. Chen, et al., Enhanced photovoltaic performance with co-sensitization of porphyrin and an organic dye in dye-sensitized solar cells, Energy Environ. Sci. 5 (2012) 6460, doi:http://dx.doi.org/10.1039/c2ee21104a.

[21] H.-P. Wu, Z.-W. Ou, T.-Y. Pan, C.-M. Lan, W.-K. Huang, H.-W. Lee, et al., Molecular engineering of cocktail co-sensitization for efficient panchromatic porphyrin-sensitized solar cells, Energy Environ. Sci. 5 (2012) 9843, doi:http://dx.doi.org/10.1039/c2ee2.

[22] J.N. Clifford, A. Forneli, H. Chen, T. Torres, S. Tan, E. Palomares, Co-sensitized DSCs: dye selection criteria for optimized device Voc and efficiency, J. Mater. Chem. 21 (2011) 1693, doi:http://dx.doi.org/10.1039/c0jm03661g.

[23] M. Kimura, H. Nomoto, N. Masaki, S. Mori, Dye molecules for simple co-sensitization process: fabrication of mixed-dye-sensitized solar cells, Angew. Chem. Int. Ed. Engl. 51 (2012) 4371–4374, doi:http://dx.doi.org/10.1002/anie.201108610.

[24] L. Jin, Z.L. Ding, D.J. Chen, Zinc octacarboxylic phthalocyanine/lutein dyads co-adsorbed nanocrystalline TiO2 electrode: enhancement in photovoltaic performance of dye-sensitized solar cells, J. Mater. Sci. 48 (2013) 4883–4891, doi:http://dx.doi.org/10.1007/s10853-013-7268-y.

[25] D. Kuang, P. Walter, F. Nüesch, S. Kim, J. Ko, P. Comte, et al., Co-sensitization of organic dyes for efficient ionic liquid electrolyte-based dye-sensitized solar cells, Langmuir. 23 (2007) 10906–10909, doi:http://dx.doi.org/10.1021/la702411n.

[26] J.-H. Yum, S.-R. Jang, P. Walter, T. Geiger, F. Nüesch, S. Kim, et al., Efficient co-sensitization of nanocrystalline TiO (2) films by organic sensitizers, Chem. Commun. (Camb). (2007) 4680–4682, doi:http://dx.doi.org/10.1039/b710759e.

[27] A. Kongkanand, R.M. Domínguez, P.V. Kamat, Single wall carbon nanotube scaffolds for photoelectrochemical solar cells Capture and transport of photogenerated electrons, Nano Lett. 7 7 (2007) 676–680, doi:http://dx.doi.org/10.1021/nl0627238.

[28] A. Kongkanand, P.V. Kamat, Electron storage in single wall carbon nanotubes Fermi level equilibration in semiconductor-SWCNT suspensions, ACS Nano. 1 (2007) 13–21, doi:http://dx.doi.org/10.1021/nn700036f.

[29] P. Du, L. Song, J. Xiong, N. Li, L. Wang, Z. Xi, et al., Dye-sensitized solar cells based on anatase TiO2/multi-walled carbon nanotubes composite nanofibers photoanode, Electrochim. Acta. 87 (2013) 651–656, doi:http://dx.doi.org/10.1016/j.electacta.2012.09.096.

[30] K.T. Dembele, G.S. Selopal, C. Soldano, R. Nechache, J.C. Rimada, I. Concina, et al., Hybrid Carbon Nanotubes–TiO 2 Photoanodes for High Efficiency Dye-Sensitized Solar Cells, J. Phys. Chem. C. 117 (2013) 14510–14517, doi:http://dx.doi.org/10.1021/jp403553t.

[31] J. Liu, Y.-T. Kuo, K.J., Klabunde, C., Rochford, J., Wu, J. Li, Novel dye-sensitized solar cell architecture using TiO2-coated vertically aligned carbon nanofiber arrays., ACS Appl. Mater. Interfaces. 1 (2009) 1645-9. http://dx.doi.org/10.1021/am900316f

[32] S.-R. Jang, R., Vittal, K.-J. Kim, Incorporation of functionalized single-wall carbon nanotubes in dye-sensitized TiO2 solar cells., Langmuir. 20 (2004) 9807-10. http://dx.doi.org/10.1021/la049022f

[33] G. te Velde, F.M. Bickelhaupt, E.J. Baerends, C. Fonseca Guerra, S.J.A. van Gisbergen, J.G. Snijders, et al., Chemistry with ADF, J. Comput. Chem. 22 (2001) 931–967, doi:http://dx.doi.org/10.1002/jcc.1056.

[34] U. Mehmood, I.A. Hussein, K. Harrabi, B.V.S. Reddy, Density functional theory study on dye-sensitized solar cells using oxadiazole-based dyes, J. hotonics Energy. 5 (2015) 053097, doi:http://dx.doi.org/10.1117/1. JPE.5.053097.

[35] U. Mehmood, I.A. Hussein, M. Daud, S. Ahmed, K. Harrabi, Theoretical study of benzene/thiophene based photosensitizers for dye sensitized solar cells (DSSCs), Dye. Pigment. 118 (2015) 152–158, doi:http://dx.doi.org/10.1016/j.dyepig.2015.03.003.

[36] R. Kavitha, L.G. Devi, Synergistic effect between carbon dopant in titania lattice and surface carbonaceous species for enhancing the visible light photocatalysis, J. Environ. Chem. Eng. 2 (2014) 857–867, doi:http://dx.doi.org/10.1016/j.jece.2014.02.016.

[37] U. Mehmood, I.A. Hussein, K. Harrabi, M.B. Mekki, S. Ahmed, N. Tabet, Hybrid TiO2–multiwall carbon nanotube (MWCNTs) photoanodes for efficient dye sensitized solar cells (DSSCs), Sol. Energy Mater. Sol. Cells. 140 (2015) 174–179, doi:http://dx.doi.org/10.1016/j.solmat.2015.04.004.

[38] L. Han, N. Koide, Y. Chiba, A. Islam, R. Komiya, N. Fuke, et al., Improvement of efficiency of dye-sensitized solar cells by reduction of internal resistance, Appl, Phys. Lett. 86 (2005) 213501, doi:http://dx.doi.org/10.1063/1.1925773.

[39] P. Joshi, L. Zhang, Q. Chen, D. Galipeau, H. Fong, Q. Qiao, Electrospun carbon nanofibers as low-cost counter electrode for dye-sensitized solar cells, ACS Appl. Mater. Interfaces 2 (2010) 3572–3577, doi:http://dx.doi.org/10.1021/am100742s.

[40] and G.C. Qifeng Zhang, Tammy P. Chou, Bryan Russo, Samson A. Jenekhe, Polydisperse Aggregates of ZnO Nanocrystallites: A Method for Energy-Conversion-Efficiency Enhancement in Dye-Sensitized Solar Cells, Adv. Funct. Mater. 18 (2008) 1654-1660.

[41] K. LEE, C. HU, H. CHEN, K. HO, Incorporating carbon nanotube in a low-temperature fabrication process for dye-sensitized TiO2 solar cells☆, Sol. Energy Mater. Sol. Cells 92 (2008) 1628–1633, doi:http://dx.doi.org/10.1016/j.solmat.2008.07.012.

[42] Y.-L. Xie, Z.-X. Li, Z.-G. Xu, H.-L. Zhang, Preparation of coaxial TiO2/ZnO nanotube arrays for high-efficiency photo-energy conversion applications, Electrochem. Commun. 13 (2011) 788–791, doi:http://dx.doi.org/10.1016/j.elecom.2011.05.003.

[43] S. Li, Y. Lin, W. Tan, J. Zhang, X. Zhou, J. Chen, et al., Preparation and performance of dye-sensitized solar cells based on ZnO-modified TiO2 electrodes, Int. J. Miner. Metall. Mater. 17 (2010) 92–97, doi:http://dx.doi.org/10.1007/s12613-010-0116-z.

[44] A.S. Nair, R. Jose, Y. Shengyuan, S. Ramakrishna, A simple recipe for an efficient TiO2 nanofiber-based dye-sensitized solar cell, J. Colloid Interface Sci. 353 (2011) 39–45, doi:http://dx.doi.org/10.1016/j.jcis.2010.09.042.